Article

A Generalized Model for the Molecular Arrangement in the Columnar Mesophases of Polycatenar Mesogens. Crystal and Molecular Structure of Two Hexacatenar Mesogens

Bertrand Donnio, Benot Heinrich, Hassan Allouchi, Jens Kain, Siegmar Diele, Daniel Guillon, and Duncan W. Bruce

J. Am. Chem. Soc., **2004**, 126 (46), 15258-15268• DOI: 10.1021/ja0471673 • Publication Date (Web): 28 October 2004

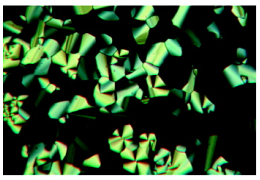
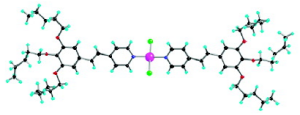
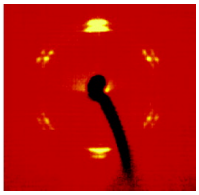

J|A|C|S
ARTICLES
Published on Web 10/28/2004

A Generalized Model for the Molecular Arrangement in the Columnar Mesophases of Polycatenar Mesogens. Crystal and Molecular Structure of Two Hexacatenar Mesogens

Bertrand Donnio,*,‡ Benoît Heinrich,‡ Hassan Allouchi,|| Jens Kain,§ Siegmar Diele,§ Daniel Guillon,‡ and Duncan W. Bruce*,†

Contribution from the Department of Chemistry, University of Exeter, Stocker Road, EXETER EX4 4QD, UK; Institut de Physique et Chimie des Matériaux de Strasbourg, GMO, CNRS-Université Louis Pasteur (UMR 7504), 23 rue des Loess, BP 43, 67034 Strasbourg Cedex 2, France; Institute of Physical Chemistry, Martin-Luther-Universität Halle-Wittenberg, Mühlpforte 1, 06120 Halle, Germany; and Laboratoire de Chimie Physique, PIMIR E.A. 2098, Faculté des Sciences Pharmaceutiques, 31 avenue Monge, 37200 Tours, France

Received May 14, 2004; E-mail: d.bruce@exeter.ac.uk; bdonnio@ipscms.u-strasbg.fr

Abstract: The columnar mesophases of two series of hexacatenar palladium(II) mesogens have been studied in detail by a combination of X-ray diffraction on aligned and unaligned samples and dilatometry. The results of these studies, combined with the results of two single crystal structure determinations, have allowed a model of the molecular arrangement in the columnar phases to be proposed. This model differs in detail from that generally accepted for the arrangement of polycatenar mesogens in columnar phases, and a new model is proposed which accounts for both new and existing data.

Introduction

The past twenty years or so have seen a revolution in the synthesis of thermotropic liquid-crystalline materials as researchers have begun to move away from the perceived wisdom of concentrating solely on rodlike and disklike molecular motifs.[1] Thus, for example, liquid crystals are now commonly found that are dendrimeric,[2] have bent cores,[3] are constructed using noncovalent bonding,[4] contain metals,[5] are bowlic in shape,[6] or rely on microphase separation to drive the formation of their mesophases.[7] Similarly, the groups of both Goodby[8] and Tschierske[9] have considered the phase diagrams of lyotropic liquid crystals, which can be considered as being controlled by interfacial curvature, and have demonstrated that the same phases could be realized through appropriately designed *thermotropic* materials. Related work by Percec and co-workers has investigated the assembly of dendron units into supramolecular species with well-defined shapes (cones, disks and spheres) which subsequently self-organize into columnar and cubic mesophases. Thus, for example, flat, tapered, half-disk, and disklike dendrons lead to cylindrical arrangements, whereas conical, half-sphere, and spheroidal dendrons lead to a spherical arrangement.[10]

In all of the above cases, a central consideration is how the molecules organize in the mesophases particularly when the molecular motif is very nonclassical. This can turn up some interesting features; for example, it is now known that spontaneous chiral resolution can be observed in certain phases of bent-core liquid crystals.[11]

One of the most interesting of the newer motifs is represented by *polycatenar* liquid crystals which are constituted by a long,

† University of Exeter.
‡ CNRS-Université Louis Pasteur.
§ Martin-Luther-Universität Halle-Wittenberg.
|| Faculté des Sciences Pharmaceutiques.

(1) Demus, D. *Liq. Cryst.* **1989**, *5*, 75−110. Goodby, J. W.; Mehl, G. H.; Saez, I. M.; Tuffin, R. P.; Mackenzie, G.; Auzély-Velty, R.; Benvegnu, T.; Plusquellec, D. *Chem. Commun.* **1998**, 2057−2070. Goodby, J. W. *Curr. Opin. Solid State Mater. Sci.* **1999**, *4*, 361−368.
(2) Ponomarenko, S. A.; Boiko, N. I.; Shibaev V. P. *Polym. Sci. Ser. A* **2001**, *43*, 1−45. Guillon, D.; Deschenaux, R. *Curr. Opin. Solid State Mater. Sci.* **2002**, *6*, 515−525. Moore, J. S. *Acc. Chem. Res.* **1997**, *55*, 13377−13394. Pesak, D. J.; Moore, J. S. *Angew. Chem., Int. Ed.* **1997**, *36*, 1636−1639. Meier, H.; Lehmann, M.; Kolb, U. *Chem.—Eur. J.* **2000**, *6*, 2462−2469.
(3) Pelzl, G.; Diele, S.; Weissflog, W. *Adv. Mater.* **1999**, *11*, 707−724.
(4) Paleos, C. M.; Tsiourvas, D. *Liq. Cryst.* **2001**, *28*, 1127−1161. Nguyen, H. L.; Horton, P. N.; Hursthouse, M. B.; Legon, A. C.; Bruce, D. W. *J. Am. Chem. Soc.* **2004**, *126*, 16−17.
(5) Donnio, B.; Guillon, D.; Deschenaux, R.; Bruce, D. W. Metallomesogens. In *Comprehensive Coordination Chemistry II: From Biology to Nanotechnology*; McCleverty, J. A., Meyer, T. J., Eds. (Fujita, M., Powell, A. K., Vol. Eds.); Elsevier: Oxford, UK, 2003; Vol. 7, Chapter 7.9, pp 357−627.
(6) Levelut, A. M.; Malthête, J.; Collet, A. *J. Phys. (France)* **1986**, *47*, 351−7. Zimmermann, H.; Poupko, R.; Luz, Z.; Billard, J. *Z. Naturforsch., A: Phys., Phys. Chem., Kosmophys.* **1985**, *40*, 149−60.
(7) For example, see: Tschierske, C. *J. Mater. Chem.* **2001**, *11*, 2647−2671. Tschierske, C. *Curr. Opin. Colloid Interface Sci.* **2002**, *7*, 69−80.
(8) West, J. J.; Bonsergent, G.; Mackenzie, G.; Ewing, D. F.; Goodby, J. W.; Benvegu, T.; Plusquellec, D.; Bachir, S.; Bault, P.; Douillet, O.; Gode, P.; Goethals, G.; Martin, P.; Villa, P. *Mol. Cryst., Liq. Cryst.* **2001**, *362*, 23−44.
(9) Cheng, X. H.; Diele, S.; Tschierske, C. *Angew. Chem., Int. Ed.* **2000**, *39*, 592−5.
(10) For example, see: Balagurusamy, V. S. K.; Ungar, G.; Percec, V.; Johansson, G. *J. Am. Chem. Soc.* **1997**, *119*, 1539−1555. Hudson, S. D.; Jung, H. T.; Percec, V.; Cho, W. D.; Johansson, G.; Ungar, G.; Balagurusamy, U. S. K. *Science* **1997**, *278*, 449−452. Ungar, G.; Percec, V.; Holerca, M. N.; Johansson, G.; Heck, J. A. *Chem.—Eur. J.* **2000**, *6*, 1258−1266. Percec, V.; Cho, W. D.; Ungar, G.; Yeardley, D. J. P. *Angew. Chem., Int. Ed.* **2000**, *39*, 1597−1602. Percec, V.; Cho, W. D.; Ungar, G.; Yeardley, D. J. P. *J. Am. Chem. Soc.* **2001**, *123*, 1302−1315. Ungar, G.; Liu, Y.; Zeng, X.; Percec, V.; Cho, W. D. *Science* **2003**, *299*, 1208−1211.

10.1021/ja0471673 CCC: $27.50

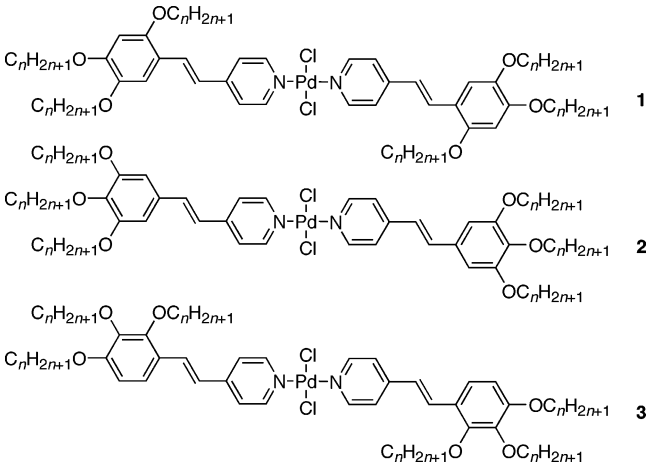

Figure 1. Structure of the hexacatenar palladium complexes.

rigid, usually aromatic core, to which at least three terminal aliphatic chains are grafted at the extremities.[12] In the majority of cases, the terminal chains are disposed symmetrically and it is found that the mesomorphism of hexacatenar mesogens (i.e. those with six terminal chains, three at each end) is dominated by the formation of columnar phases, while certain isomers of tetracatenar mesogens can form, in the same homologous series, nematic, smectic C, cubic, and columnar phases.[13] The driving forces for such diverse mesomorphism within a single homologous series have been discussed and there has been substantial interest in the crossover between lamellar and columnar phases, related in part to an understanding of the molecular organization within cubic and columnar phases.[14]

Previously,[15] we reported on three series of isomeric hexacatenar metallomesogens shown in Figure 1 whose mesomorphism had been assigned on the basis of optical microscopy. We found that the palladium complexes based on the 2,4,5-trisubstituted stilbazoles (**1**-*n*) were not mesomorphic, while columnar phases were observed for the complexes based on the 3,4,5-trisubstituted stilbazoles (**2**-*n*) and those based on the 2,3,4-trisubstituted analogue (**3**-*n*) (Supporting Information, Figure S1). (The nomenclature **1**-*n*, **2**-*n*, and **3**-*n* implies compound **1**, **2**, and **3** with *n* carbon atoms in the terminal chains.) In the case of complexes **2**, we reported that, for $n < 9$, the materials were nonmesomorphic, while, for $n \geq 9$, a single columnar phase was observed which was assigned as Col_h on the basis of optical microscopy. In the case of **3**, we found that for, $n = 6$, the materials were not mesomorphic, while, for $n = 8$, 10, 12, and 14, it was possible to identify two mesophases by optical microscopy. The mesophase found to higher temperature was assigned as Col_h, but the lower-temperature phase was not identified and transitions between these two phases were not observed by DSC.

We have subsequently undertaken a detailed investigation of the mesomorphism of **2** and **3** by X-ray diffraction and dilatometry, the results of which are now reported. It will be seen that the inferences drawn from these studies appear initially to be at odds with the accepted description of the molecular arrangement within the columnar phases of polycatenar systems, leading to the proposal of a revised and general model which accommodates both the new and the existing data. Further, single-crystal X-ray structural determinations have been possible for one homologue of **2** and one of **3**; these are the first single-crystal structures of hexacatenar compounds.

Results

Single-Crystal Structure Determinations. Suitable crystals of **2**-5 and **3**-8 were grown with some difficulty at room temperature from toluene solution by slow evaporation and were very fragile. Crystal data are given in the Supporting Information (Table S1), while other data are found via the cif file in the Supporting Information.

The molecules lie on a center of symmetry (*P*-1 with $Z = 2$ of **3**-8 and P_{21}/c with $Z = 4$ for **2**-5), and the asymmetric unit corresponds to the half of a molecule with the Pd atoms in the (0, 0, 0) for **3**-8 and (1, 1, 0) for **2**-5. Views of the two structures are given in Figures 2 and 3, while labeled ellipsoid[16] representations are given in the accompanying Supporting Information (Figures S2 and S3).

The thermal motion factors of the polyaromatic central core in both compounds are rather low, while those of the terminal alkyloxy chains are slightly higher for **2**-5 and higher again for **3**-8, increasing substantially along the chains. In **2**-5, therefore, the rather limited number of observed reflections, according to the high thermal motion of alkoxy chains, may explain the relatively high *R* factor.

In each case, the polycyclic central core has two quasi-planar consecutive ring groups (N1 to C6) and (C9 to C14), and the dihedral angle between them is equal to 23.8(1)° and 10.6(9)° for **3**-8 and **2**-5, respectively. The core conformations for both molecules are rather similar.

The lengths of the polyaromatic central cores (distance O33...O33a: homologue O33 relative to the center of symmetry) are found to be 25.46 and 25.39 Å, respectively, for **3**-8 and **2**-5, and total molecular lengths (distance C41...C41a and C38...C38a, respectively, for **3**-8 and **2**-5, C38a and C41a: homologues C38 and C41 relative to the center of symmetry) were evaluated as 44.46 and 34.05 Å, respectively. However, if the bulkiness of the terminal CH_3 [$r(CH_3) = 2.0$ Å] group is taken into account, the total length, $d = [d(\text{C41...C41a}) + 2r_{CH_3}]$, is actually 48.46 and 38.05 Å for **3**-8 and **2**-5, respectively.

A. Arrangement of the Chains. The three alkoxy chains of **3**-8 are labeled as indicated in Figure 3. The O−C−C−C torsion angles, at the beginning of each alkyloxy chain, are equal to 168°, −50°, and 178° for chains 1, 2, and 3, respectively; the corresponding lengths of the chains are 8.75, 8.55, and 9.90 Å, respectively. Alkoxy chain 3 is completely extended with C−C−C−C angles deviating from 180° by less 10°, while alkoxy chains 1 and 2 are partly extended with a torsion angle around

(11) Niori, T.; Sekine, F.; Watanabe, J.; Furukawa, T.; Takezoe, H. *J. Mater. Chem.* **1996**, *6*, 1231. Link, D. R.; Natale, G.; Shao, R.; Maclenan, J. E.; Clark, N. A.; Korblova, E.; Walba, D. M. *Science* **1997**, *278*, 1924−7.
(12) Malthête, J.; Nguyen, H. T.; Destrade, C. *Liq. Cryst.* **1993**, *13*, 171−187. Nguyen, H. T.; Destrade, C.; Malthête, J. *Adv. Mater.* **1997**, *9*, 375−388. Nguyen, H. T.; Destrade, C.; Malthête, J. In *Handbook of Liquid Crystals*; Demus, D., Goodby, J., Gray, G. W., Spiess, H.-W., Vill, V., Eds.; Wiley-VCH: Weinheim, 1998; Vol. 2B, p 865. Gharbia, M.; Gharbi, A.; Nguyen, H. T.; Malthête, J. *Curr. Opin. Colloid Interface Sci.* **2002**, *7*, 312−325.
(13) Rowe, K. E.; Bruce, D. W. *J. Mater. Chem.* **1998**, *8*, 331−342.
(14) For example, see: Fazio, D.; Mongin, C.; Donnio, B.; Galerne, Y.; Guillon, D.; Bruce, D. W. *J. Mater. Chem.* **2001**, *11*, 2852−2863 and references therein.
(15) (a) Donnio, B.; Bruce, D. W. *J. Chem. Soc., Dalton Trans.* **1997**, 2745−2755. (b) Smirnova, A. I.; Fazio, D.; Iglesias, E. F.; Hall, C. G.; Guillon, D.; Donnio, B.; Bruce, D. W. *Mol. Cryst. Liq. Cryst.* **2003**, *396*, 227−240.
(16) Spek, A. L. *Platon99, Program for Drawing Crystal and Molecular Diagrams*; University of Utrecht: Netherlands, 1999.

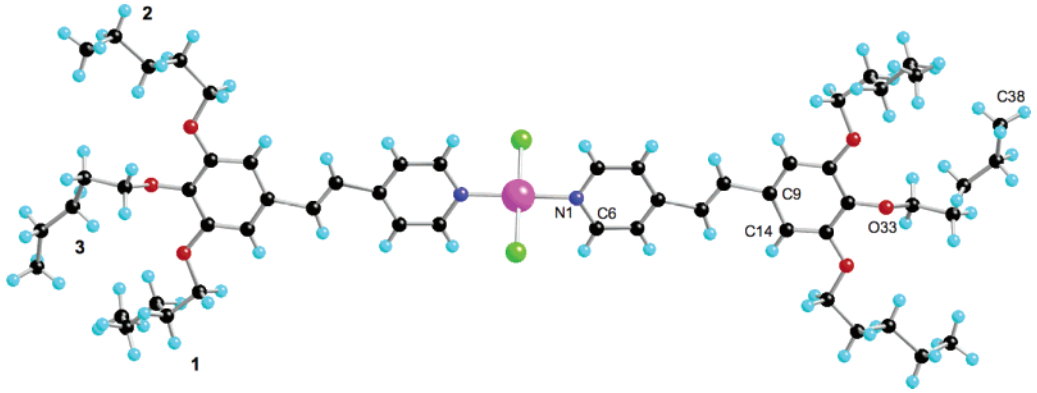

Figure 2. Molecular Structure of **2**-5 including chain numbering.

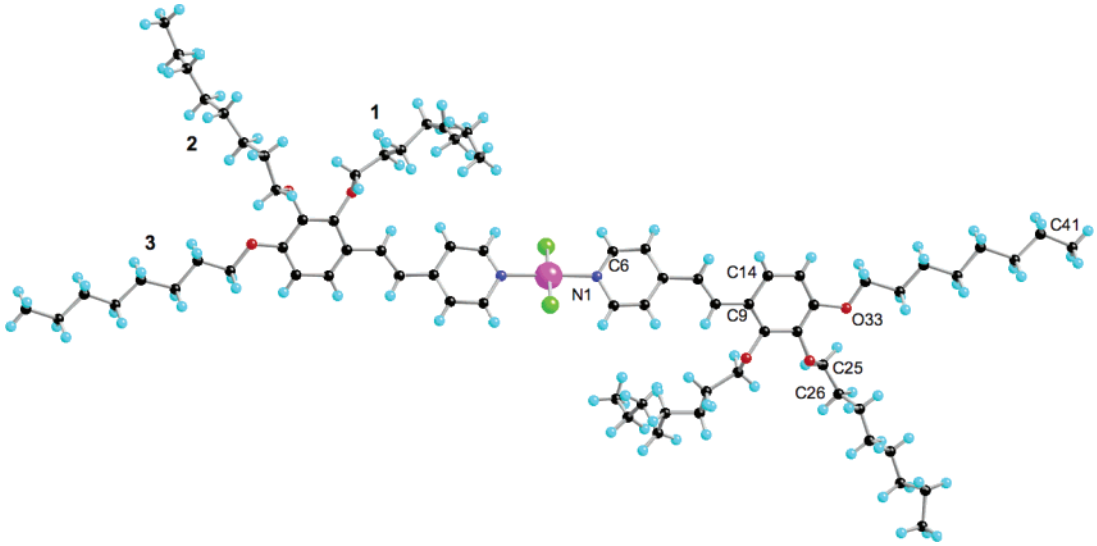

Figure 3. Molecular Structure of **3**-8 including chain numbering

C19−C20 (chain 1; see Supporting Information, Figure S2) and C25−C26 (chain 2) close to −70.58° and −50.44°, respectively. The mean plane of the central core and alkyloxy chains is close to 77°, 84°, and 15°, respectively, for chains 1, 2, and 3; the mean planes of chains 1 and 2 make an angle close to 74°, while the mean planes of chains 2 and 3 makes an angle close to 88°.

The three alkoxy chains of **2**-5 are labeled as indicated in Figure 2. The O−C−C−C torsion angles, at the beginning of each alkyloxy chain, are equal to 69°, 63°, and 59° for chains 1, 2, and 3, respectively; the corresponding lengths of the chains are 5.37, 5.16, and 5.23 Å, respectively. Alkyloxy chains 1 and 2 are completely extended with C−C−C−C angles deviating from 180° by less 10°, while alkoxy chain 3 is in a gauche conformation. The mean plane of the central core and alkyloxy chains is close to 60°, 40°, and 25°, respectively for chain 1, 2, and 3; the mean plane of chains 1 and 2 make an angle close to 90°, while the mean planes of chains 2 and 3 make an angle close to 48°.

B. Molecular Packing and Arrangement. The projection of the structure along the *a* axis for **3**-8 and the projection of the structure along the *b* axis for **2**-5 are shown in the Supporting Information (Figures S4 and S5, respectively). The polyaromatic cores are aligned and strictly parallel, and so the cohesion of the crystal is due almost entirely to van der Waals forces between the polyaromatic central cores related by the centers of symmetry. There are very few interactions involving alkoxy chains between neighboring molecules. The molecules arrange to give two-dimensional sheets parallel to the plane (*xoy*) with a thickness of about 23.4 Å for **3**-8 and 34.2 Å for **2**-5, corresponding to the length of the *c* parameter. The interactions between sheets involving the terminal methyl groups are very weak.

The molecular arrangement is typical of a lamellar structure with segregation of the aliphatic chains and central polyaromatic cores into distinct sublayers.

Dilatometry. To gain a better understanding of the molecular organization within the columns, measurements of molecular volume and certain other parameters were undertaken as a function of *T* and *n*. Dilatometry allows the specific molecular volume to be obtained and, combined with the results of the X-ray experiments, enables further structural information to be extracted. Details of the technique may be found in ref 17. However, before proceeding to elaborate on the structural aspects of the mesomorphism, it is necessary to consider certain relationships which underpin the discussion.

Thus, for a given columnar "portion" of height *h*, it is possible to define the volume of the corresponding cell as

$$V_{\text{cell}} = hs \qquad (1)$$

where V_{cell} is the volume of the repeat unit (cell) and *s* is the

columnar cross section calculated from the lattice parameters obtained from X-ray diffraction. In the same repeat unit of the column, it is also possible to define the number of molecules contained within the cell, N_{cell}, according to

$$N_{cell} = \frac{hs}{V_{mol}} \quad (2)$$

where V_{mol} is the volume of one molecule.

Further, it is now well established that the volume of a single molecule, V_{mol}, can be expressed in terms of two components,[18] the rigid part, V_{ar}, and the chains, V_{ch},[19] according to

$$V_{mol} = V_{ar} + V_{ch} \quad (3)$$

And hence, the volume fraction of the rigid part,[20] f_{ar}, can be expressed as

$$f_{ar} = \frac{V_{ar}}{V_{mol}} \quad (4)$$

Now, rearranging eq 2 allows the parallel expressions 5a and 5b to be derived:

$$NV_{mol} = hs \quad (5a)$$

$$NV_{ar} = hs_{ar} \quad (5b)$$

If the ratio of 5b/5a is taken, it is then possible to write

$$\frac{V_{ar}}{V_{mol}} = \frac{s_{ar}}{s} = f_{ar} \quad (6)$$

Something crucial in understanding the use of these equations is that they are derived from macroscopic observations and are averaged over effectively an infinite time span compared to molecular motion. Thus, while the core of these mesogens is effectively rectangular in shape, the time scale for data collection is such that s_{ar} actually refers to a circular or elliptical, two-dimensional area projected onto the plane perpendicular to the column direction. The diameter of this circle will depend on the relative orientation of the core within the column so that if the core is perpendicular to the column axis, the circle diameter will be comparable to the core length. The diameter will then decrease with any tilting of the core, reflecting the reduced projection of the core onto the plane normal to the column direction.

Thus, from expression 3 and the experimentally determined molecular volumes,[21] it is possible to estimate V_{ar} and, therefore, the volume fraction f_{ar}, since V_{CH_2} may be calculated as discussed elsewhere.[19]

(17) Guillon, D.; Skoulios, A. *Mol. Cryst. Liq. Cryst.* **1977**, *39*, 139−157.
(18) (a) Guillon, D. *Struct. Bonding* **1999**, *95*, 41−82. (b) Guillon, D.; Donnio, B.; Bruce, D. W.; Cukiernik, F. D.; Rusjan, M. *Mol. Cryst. Liq. Cryst.* **2003**, *396*, 141−154.
(19) $V_{ch} = 6(nV_{CH_2} + \Delta V_{CH_3})$, where 6 corresponds to the number of chains per molecule, n, the number of methylene groups per chain, V_{CH_2}, the volume of one methylene unit ($V_{CH_2} = 26.5616 + 0.020\,23T$), and ΔV_{CH_3}, the volume contribution of the end group $\Delta V_{CH_3} = 27.14 + 0.017\,13T + 0.000\,418\,1T^2$).
(20) For example, see: Morale, F.; Date, R. W.; Guillon, D.; Bruce, D. W.; Finn, R. L.; Wilson, C.; Blake, A. J.; Schröder, M.; Donnio, B. *Chem.—Eur. J.* **2003**, *9*, 2484−2501.
(21) $V_{ar}^{234} = 525.1$, $V_{mol}^{234} = (669 + 0.42T) + n(159.4 + 0.12T)$; $V_{ar}^{245} = 528.5$, $V_{mol}^{345} = (672.4 + 0.42T) + n(159.4 + 0.12T)$ in Å^3 (T in °C).

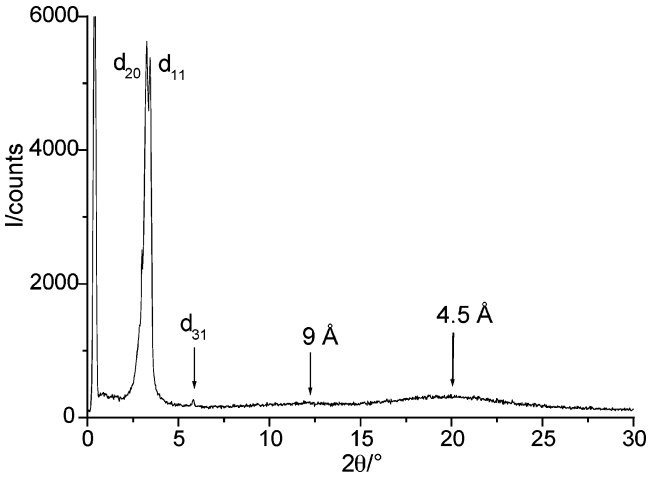

Figure 4. X-ray diffraction pattern in the Col_r phase of **3**-10 at 100 °C.

X-ray Diffraction. A. Powder Samples. Data were collected for all the samples under discussion throughout the mesomorphic range. The collection of such a large amount of data is necessary to complement the data obtained from the dilatometry experiments, hence allowing the proposal of a model for the mesomorphism of these complexes which takes into account the dependence on isomer, chain length, and temperature. The X-ray results will be discussed in detail below, but it is helpful first to indicate the general form of the data obtained from which the conclusions are drawn. Thus, at high angles ($2\theta \approx 20°$) a broad, diffuse scattering halo was observed corresponding to a spacing of ∼4.5 Å which relates to the liquidlike order of the aliphatic chains. In the small-angle region ($0 < 2\theta < 5°$), several sharp and intense reflections were observed corresponding to the fundamental, harmonics, and higher orders of diffraction and indicative of the two-dimensional lattice of the columnar phases. Analysis of the *d*-spacings arising from these data allow the two-dimensional symmetry of the mesophase to be identified. Another less intense, but diffuse, halo was observed at intermediate angles ($2\theta \approx 10°$), corresponding to a distance which varied in complexes of series **2** (9 to 10 Å), but was constant for series **3** (ca. 9 Å). We will return to this reflection later. An example of the X-ray pattern of a Col_r phase is included as Figure 4, while patterns for the Col_h phase are found in the Supporting Information (Figure S6).

i. Columnar Hexagonal Phase: The identity of the columnar hexagonal phase was confirmed unambiguously for complexes **2** and **3**. Two or three sharp, small-angle reflections with reciprocal spacings in the ratio 1, $\sqrt{3}$, and $\sqrt{4}$ corresponding to the indexation $(hk) = (10)$, (11), and (20) were observed in the patterns, and these are characteristic of a two-dimensional, hexagonal lattice (Figure 5a). These results are consistent with the optical textures observed on cooling from the isotropic liquid (see Supporting Information, Figures S7−S10 for illustrative optical micrographs).

ii. Columnar Rectangular Phase: As suggested previously for compounds **3** by optical microscopy, the mesophase appearing below the hexagonal columnar phase was found to possess a two-dimensional, rectangular lattice. The presence of two sharp peaks (fundamental reflections), one corresponding to the (20) reflection and the other to the (11) and $(1\bar{1})$ pair, are indeed characteristic of a rectangular lattice. In some cases, higher orders of diffraction could be observed (although at much

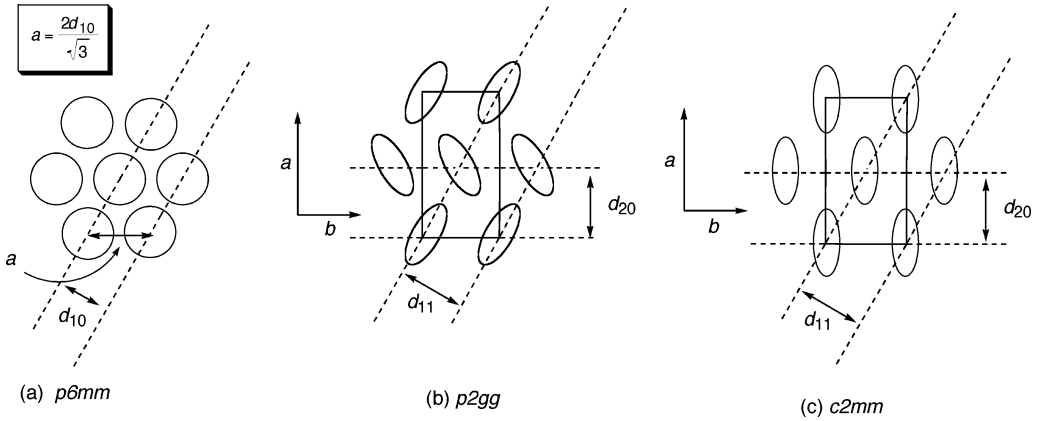

Figure 5. Representation of the arrangement of the columns in the (a) *p*6*mm*, (b) *p*2*gg*, and (c) *c*2*mm* plane group.

lower intensities), further confirming the rectangular symmetry. However, as there are more than one rectangular plane group, it is of interest to determine which particular Col_r phase is present.

We will discuss a model for the arrangement of the molecules in the columns later, but for now we can consider the model applicable to columnar phases of disklike molecules which stack up above one another. Where the disks are perpendicular to the column axis, then a circular cross section is projected, while when the disks are tilted, the cross section is elliptical. Adopting such a model for the columnar phases of these materials leads to two possible two-dimensional groups for the Col_r phase, namely the *c*2*mm* and the *p*2*gg* planar groups.[22] These are shown along with *p*6*mm* (Col_h) in Figure 5.

In the case of *c*2*mm* (Figure 5c), the figure shows that the lattice may be represented by columns with an elliptical cross section and the long axis of the ellipses are oriented along an unique direction perpendicular to the columnar axis i.e. the **a** direction (arbitrary choice). In the other situation (Figure 5b, *p*2*gg*), these axes are oriented alternately along two different directions (herringbone packing), both perpendicular to the columnar axis. The lattice parameter $\mathbf{a_r}$ is, in both cases, connected directly to the d_{20} spacing ($\mathbf{a_r} = 2\ d_{20}$).

In the case of powders, the distinction between the centered *c*2*mm* and the *p*2*gg* lattices depends on the number of reflections obtained, allowing the specific conditions of the (*hk*) reflections to be tested. For *p*2*gg* symmetry, there exists the condition that $h0 = 2n$ and $0k = 2n$, whereas, in *c*2*mm* symmetry, all the (*hk*) reflections must additionally satisfy the condition $h + k = 2n$, so that the presence of forbidden reflections ($h + k = 2n + 1$) excludes *c*2*mm* symmetry.

However, in most cases, the fundamental reflections (20) and (11)/($1\bar{1}$) are normally intense, and the higher order reflections, very weak or absent, so that discrimination between the two symmetries is often not possible using powder patterns alone.

This was the case with the present materials, and so only one peak was observed in addition to the fundamentals and their first harmonics. As the smallest-angle member of the higher-order reflections, (31) or (02), is allowed in both plane groups, then discrimination was not possible.

B. Oriented Samples. Where powder patterns are insufficient, oriented, monodomain samples can provide the necessary additional information, but these are often not easily obtained. Bouligand[23] and later Cheng et al.[24] have shown that well-ordered samples can be obtained when using uncovered droplets. The experiment consists of depositing the compound onto a glass slide which is placed on a hot stage and heated into the isotropic phase. Slow cooling favors the nucleation of liquid crystal domains with specific orientations at both the substrate−liquid crystal and air−liquid crystal interfaces. In the particular case of columnar mesophases, the columns will preferentially lie horizontally to the glass slide. Thus, in an attempt to clear up this ambiguity in plane group assignment, this technique was used on two representative samples, namely **2**-10 and **3**-10. The X-ray diffraction patterns are shown in Figure 6.

i. Columnar Hexagonal Phase: The alignment of the columnar domains was obtained spontaneously by cooling slowly from the isotropic phase a droplet of the material deposited onto a glass plate. Thus, for the (10)/(01)/($1\bar{1}$) reflection ring, similar spot patterns are obtained for both complexes, revealing the alignment obtained (Figure 6a, c). Moreover, both patterns are composed of six spots located every 60° on the ring, with two lying on the meridian. The intensity of these two spots was higher than that of the other four, but the intensity ratio changes significantly when the sample stage is rotated. Actually, the spots on the meridian occur from the superposition of two patterns from differently aligned domains:

(1) those domains with the columnar axis parallel to the beam, which give six spots corresponding to the reflection by all three plane families;

(1) the domains with the columnar axis perpendicular to the beam, which give two spots corresponding to the reflection by the (10) family of planes parallel to the beam.

The exclusive observation of these spots therefore shows that the monodomains are aligned with the columnar axis, and an edge of the two-dimensional lattice lies horizontally to the air−sample interface. The superposition of both patterns shows that, within the plane parallel to this interface, there is no orientation of the monodomains, which certainly form developable domains.[23,25]

ii. Columnar Rectangular Phase: In general, on cooling from a monodomain of the hexagonal phase, it is possible to obtain several domains of a rectangular phase, the increase in

(22) Levelut, A. M. *J. Chim Phys.* **1983**, *80*, 149−161.

(23) Bouligand, Y. *J. Phys.* **1980**, *41*, 1307−1315.
(24) For example, see: Cheng, X.; Prehm, M.; Kumar Das, M.; Kain, J.; Baumeister, U.; Diele, S.; Leine, D.; Blume, A.; Tschierske, C. *J. Am. Chem. Soc.* **2003**, *125*, 10977−10996.
(25) Oswald, P.; Kléman, M. *J. Phys.* **1981**, *42*, 1461−1472.

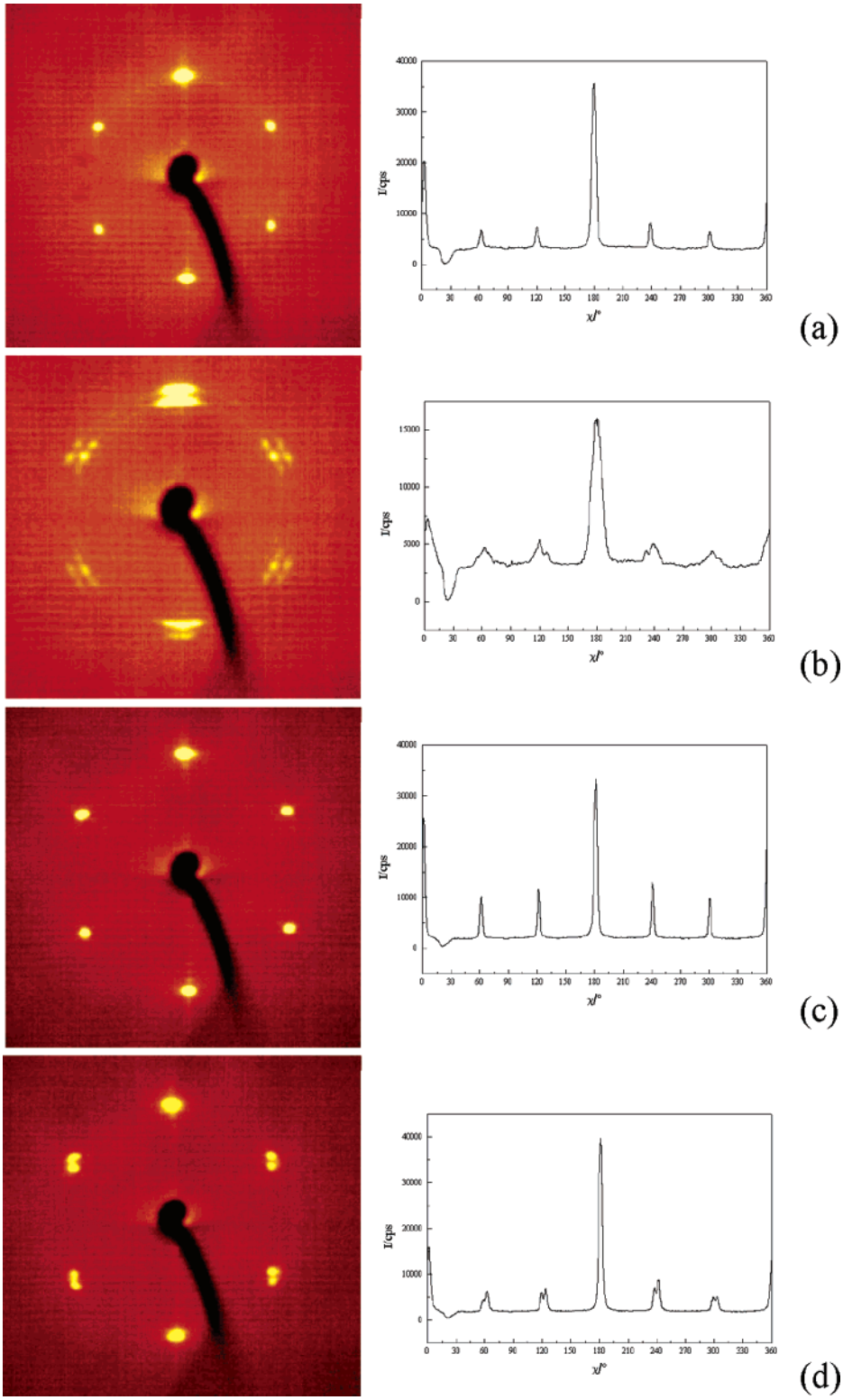

Figure 6. Oriented patterns of Col_h and Col_r phases of **2**-10 at (a) 104 °C (Col_h) and (b) 82 °C (Col_r) and of **3**-10 at (c) 147 °C (Col_h) and (d) 110°C (Col_r), respectively, along with the X-scans.

the number of Bragg spots corresponding to many different monodomains.

In the case of compound **2**-10, the monodomains with the columnar axis parallel to the beam split into six different orientations, whereby one of both reciprocal (11) directions in the Col_r phase is parallel to one of the three reciprocal (10) directions in the Col_h phase. The six monodomain orientations occur with similar probability, as shown by the relative intensity of the spots. In other words, as the reciprocal (11) directions of the rectangular network are parallel to the (10) directions of the hexagonal network, theoretically there is a maximum of six possible directions (two (11) directions × three (10) directions). It is, therefore, easy to reconstruct reciprocal space as shown in Figure 7a, which corresponds fairly well to the experimental

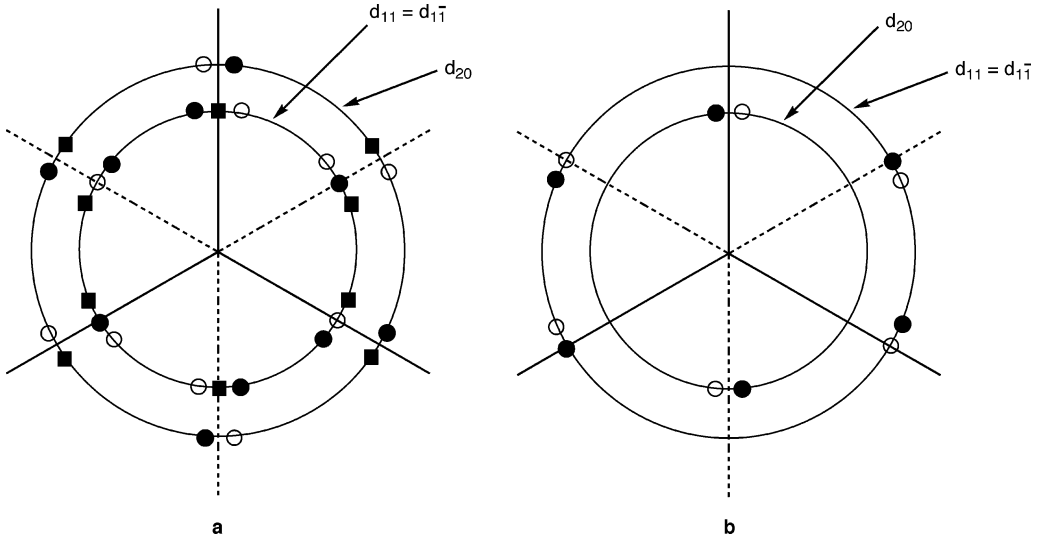

Figure 7. Patterns of the Col_r monodomains with columnar axis parallel to the beam. (a) Case of **2**-10: $3 \times 2 = 6$ orientations of the Col_r monodomains obtained from a single orientation of the Col_h monodomains. (b) Case of **3**-10: 2 orientations of the Col_r monodomains obtained from a single orientation of the Col_h monodomains.

data. Thus, it is possible to distinguish the six networks; the nodes common to both hexagonal and rectangular networks are shown in black.

In the case of compound **3**-10, the monodomains with the columnar axis parallel to the beam split into just two different orientations (Figure 7b). As for compound **2**-10, one of the reciprocal (11) directions in the Col_r phase is parallel to one of the reciprocal (10) directions in the Col_h phase, but only monodomains with the $\mathbf{a_r}$ edge perpendicular to the air−sample interface are obtained; i.e., it seems that the sides of the rectangle are parallel to the sides of the hexagonal lattice, which gives, a priori, three main orientations. Nonetheless, it appears that the *hk*0 planes of the three networks do not meet exactly, and so simultaneous observation of the Bragg spots is not possible. Stricto sensu, the diffraction patterns obtained for these complexes do not allow unequivocal identification of the plane group of the Col_r phases, but on the basis of molecular symmetry as well as the arguments developed above, we assign **2** as showing a Col_r phase with a *p*2*gg* symmetry, whereas the lattice of the Col_r of **3** is centered and the symmetry is, therefore, *c*2*mm*.

Discussion

Variation of Structural Parameters with Chain Length and Temperature. The variation in the lattice parameters as a function of chain length and reduced temperature for complexes **3** is shown in Figure 8, while the same data for complexes **2** are found in the Supporting Information (Figure S11). (The reduced temperature, T^*, is defined here as $T^* = 1 - T/T_{cl}$, where T_{cl} is the clearing temperature.) The figures show clearly that there is the expected monotonic increase in the lattice parameter as the chain length increases and also that the lattice parameters of the phases are appreciably greater for complexes **2** compared to complexes **3**; further, for any given material, the lattice parameter is almost temperature-independent. An important observation is that, for complexes **3** (Figure 8), the magnitude of the rectangular *b* parameter and the hexagonal *a* parameter are the same and show almost no variation with temperature or through the transition.

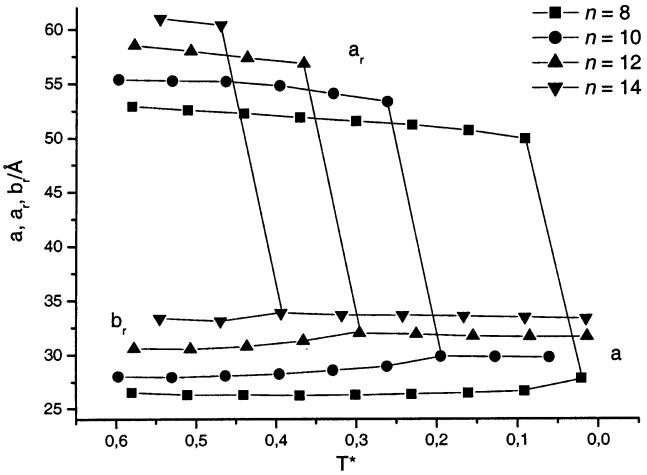

Figure 8. Variation of **a**, $\mathbf{a_r}$, and $\mathbf{b_r}$ with T^* of the Col_h and Col_r phases of **3**.

However, it is significant that, in considering only the hexagonal phase for now, the lattice parameter, *a*, which is the diameter of an individual column, is very much less than the length of an individual molecule. Thus, using the data for **2**-12 and **3**-12, values of $a = 39.3$ Å and 32.1 Å, respectively, are found, whereas calculating the molecular length (extrapolating from the structure of **3**-8) gives 53.8 Å for a mesogen with a dodecyloxy chain in the 4-position. This discrepancy will be discussed later.

The behavior of the lattice spacings at the transition from the Col_h to the Col_r phase in general takes a common form which is exemplified by Figure 9 which shows data for **3**. The corresponding data for **2** are found in the Supporting Information (Figure S12) and are of a similar form. Thus, there is some convergence in d_{20} and d_{11} as the transition is approached, which is modest for **2**-10 and more pronounced for **3**-10, although in both cases it seems that the extent of the change is greater in the reflection derived from the larger spacing (d_{11} for complexes **2** and d_{20} for complexes **3**).

Considering these data (Figures 8 and 9) for complexes **3**, information is provided concerning the nature of the transition.

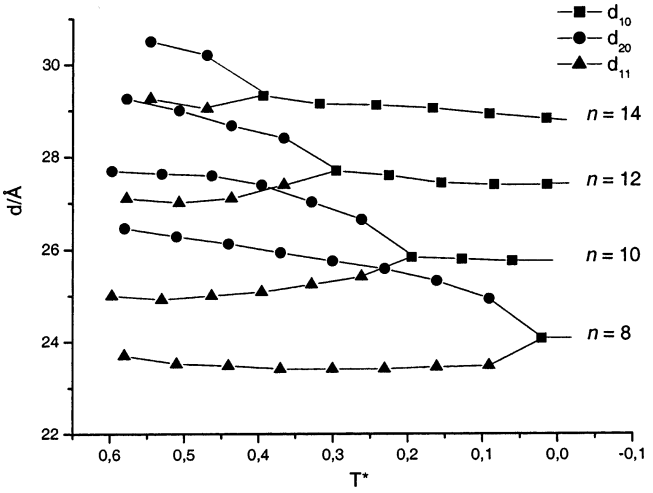

Figure 9. Variation in *d* with *T** for **3**.

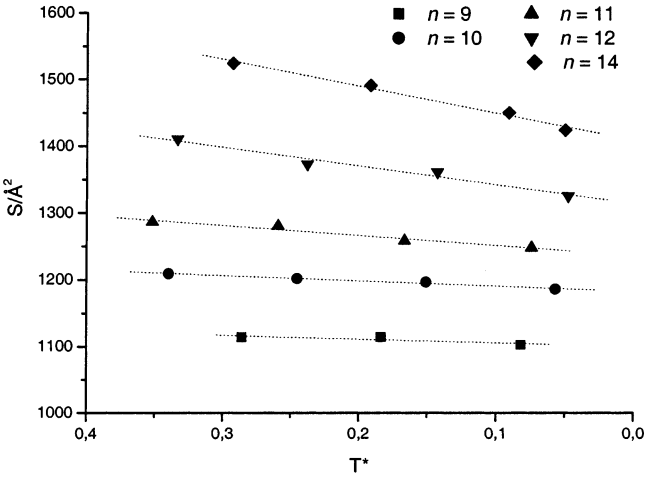

Figure 10. Variation of *S* with *T** of the Col_h and Col_r phases of **2**.

Thus, consideration of Figure 5 shows that on transition from the *p*6*mm* hexagonal phase to the *c*2*mm* rectangular phase, the d_{10} reflection of the hexagonal becomes split into the d_{20} and d_{11} reflections of the rectangular phase, and the data in Figure 8 show that the *a* parameter of the *p*6*mm* phase and the *b* parameter of the *c*2*mm* phase are the same. Bringing these two sets of observations together, it is possible to deduce that the hexagonal−rectangular transition in **3** arises solely due to an elongation along what becomes the *a* direction of the rectangular phase. A similar analysis for complexes **2** shows that the hexagonal-to-rectangular transition requires both an elongation in *a* and a contraction in *b*.

Moreover, the packing appears obviously different for both series in the Col_r phase, as the rectangular networks correspond to opposite deformations of the hexagonal networks: the *a*/*b* ratio is smaller than $\sqrt{3}$ for the series **2** but larger than $\sqrt{3}$ for the series **3**.

Turning now to the columnar area, *s*, there is a large difference between *s*(**2**) and *s*(**3**) (Figures 10 and 11), suggesting that the number of molecules per unit length is different within the columns formed by the complexes. Thus, while the values of *s*(**2**) are in the approximate range 1100 to 1500 Å^2, values of *s*(**3**) are found between 700 and 1000 Å^2. Note that these figures also show that the temperature dependence of *s* is much

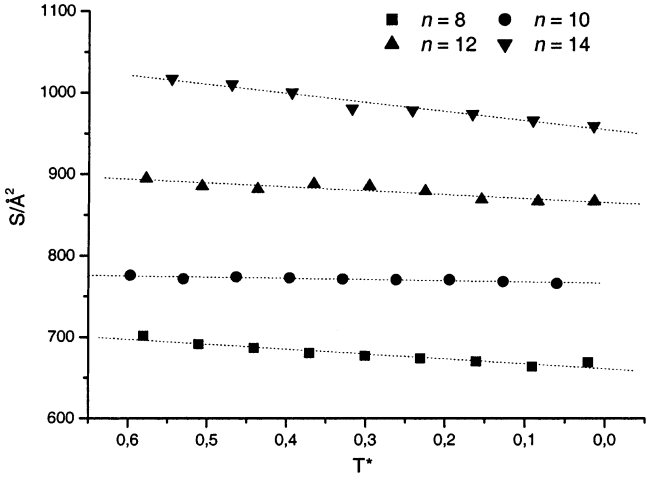

Figure 11. Variation of S with *T** of the Col_h and Col_r phases of **3**.

less for **3** than for **2**. The transition between the Col_h and Col_r phases is continuous, as there is little or no change in *s* across the transition.

This discussion can be extended to consider the behavior of s_{ar} alone, as use of eq 6 allows s_{ar} to be evaluated as V_{mol} is measured and V_{ar} can be evaluated having calculated V_{CH_2}.[21] Thus, for both **2** and **3**, s_{ar} decreases slightly with increasing temperature, and from the values of s_{ar}, it is possible to calculate the effective diameter of the core projected onto the column normal using the arguments presented above. Using **2**-12 and **3**-12 at 100 °C at which temperature both complexes are in the Col_h phase, s_{ar} is found to be 260 Å^2 and 168 Å^2, respectively giving effective column "core" diameters of 18.2 and 14.6 Å, respectively. Now, from the crystal structure determinations above, the length of the molecular core (taken to include the oxygen of the alkoxy chain in the 4-position) is 25.5 Å, and hence it is possible to calculate a tilt angle for the core in each case with respect to the columnar axis. Thus, it is found that for **2**-12 this is 44.4°, while for **3**-12 it is 57.4°. It is then possible to calculate a global tilt angle for the complexes as a whole using a calculated value of 53.8 Å for the molecular length (obtained by extrapolating from the crystal structure of **3**-8 for a mesogen with the dodecyloxy chain) and the *a* value for the Col_h phase (39.3 and 32.1 Å for **2**-12 and **3**-12, respectively) which turns out to be 43.2° for **2**-12 and 53° for **3**-12. In both cases, the global and core tilt angles are quite close to each other, although in the latter case, the deviation is a little more significant, perhaps suggesting that the chains are not organized in a coplanar manner with the core. However, it is crucial here to understand that this model allows for orientation of the molecules in a particular direction within the columns with a particular, average tilt, with an alternation of the tilt direction as indicated in Figure 12. While the average tilt will be as indicated above, clearly there will be local variation (driven primarily by the mobility of the chains) which will ensure that this tilting is not correlated strongly throughout the entire length of the column so that a mesophase, and not a crystal phase, results.

With these data now in hand, it is possible to employ eq 2 to consider how many molecules, N_{col}, are present in a given length of column, *h*. Of course, *h* can be chosen arbitrarily, but in the calculation a value of 9 Å has been assumed for **3** corresponding

Figure 12. Schematic figure to indicate how the columns may accommodate tilting molecules; color-coding is used simply to identify the different tilt directions. Note that the diagram is not drawn to imply any particular number of molecules occupying the breadth of a column.

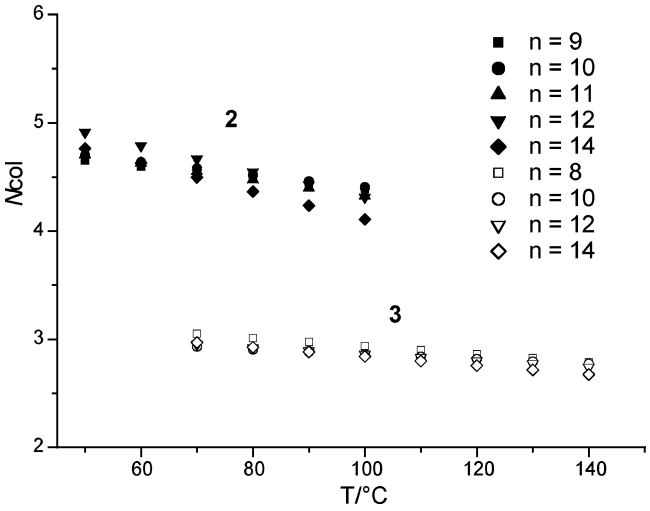

Figure 13. Number of complexes **2** and **3** calculated for a slice 9 Å thick.

to the broad signal seen in the X-ray diffraction patterns; the same value of 9 Å was also selected for compounds **2**. In selecting this value, it is not necessarily intended to imply that 9 Å corresponds to a defined columnar repeat distance, but nevertheless the data do suggest that there is a periodicity at this distance and the breadth of the signal suggests that the correlation persists over several molecules. It is also interesting to note that several previous studies of metallomesogens by X-ray diffraction have shown a similar feature at about this spacing,[20] although at this stage, no conclusion is drawn from this similarity.

Evaluating N_{col} in this way and plotting as a function of temperature leads to the plots shown in Figure 13. Thus, for complexes **2**, N_{col} takes the value of 4−5 for a 9 Å column height (higher number for higher *n*-values), while, for **3**, the value is 3. Note that, for **2**, there is a small apparent decrease in N_{col} with *T* which is consistent for all *n*, while, for **3**, N_{col} is effectively almost independent of both *T* and *n*.

Toward a Model for the Columnar Phase. The studies described above have confirmed the identity of the Col_h phase for both complexes **2** and **3** and allowed the previously[15] unidentified mesophase below Col_h in **3** to be identified as Col_r. Further, they have shown the presence of a Col_r phase below the Col_h phase in complexes **2** ($n = 9, 10, 11$) where microscopy and DSC has suggested previously that there was a single phase,[15] and the symmetry of the two Col_r phases has been identified; Table S2 (Supporting Information) shows the revised transition temperatures for these complexes.

The major questions posed by these data are as follows. First, the situation exists whereby the column diameter in the Col_h phase (equivalent to the hexagonal lattice parameter, *a*) is significantly less that the molecular length, *l*, assuming the chains to be in the all-trans conformation. How can this be understood given that the *p*6*mm* symmetry of the Col_h phase requires the columns to be of circular cross section perpendicular to the column direction? Second, the data show that the columnar cross section, *s*, does not change significantly through the *p*6*mm*-to-*c*2*mm* and *p*6*mm*-to-*p*2*gg* transition and that neither transition could be detected by DSC. Given that columns which exhibit an elliptical cross section perpendicular to the column direction are required, what is the nature of the transition? Third, is it possible to propose a general model for the arrangement of the polycatenar molecules in the columns of these phases which is consistent with the available data?

In considering the case of the Col_h phase and the need, on symmetry grounds, for the column to have a circular cross section perpendicular to the column direction, it is helpful to recall the situation found in the columnar phases of discotic molecules. Thus, in this case (Figure 14a), the molecules are considered to be rotating freely about the column axis, with respect to which they are oriented perpendicularly, giving rise to a circular cross section when projected onto the plane perpendicular to the column axis.[22] However, in the Col_r phase (Figure 14b), discotic molecules project an elliptical cross section onto the plane perpendicular to the column axis, and to achieve this, they must tilt within the column. Now, the polycatenar mesogens under study (Figure 1) cannot be regarded as circular disks, and so their shape is approximated by an ellipse. A similar argument can then be applied (Figure 14c) for if the ellipses are tilted, then at some angle which depends on the relative magnitude of the elliptical axes *a* and *b*, they will describe a circular cross section in a plane perpendicular to the propagation (column) axis. This argument requires only that the width of the column is determined by the length of the mesogen at whatever angle it subtends within the column.

Now, the calculations above for series **2** and **3** have shown that isomerically related molecules tilt to rather different degrees and yet, as both show a Col_h phase, this arrangement must allow a circular cross section to arise; this would seem to be an uncanny coincidence. However, this can be understood by first recognizing that the Col_h phase exhibits hexagonal symmetry which is an efficient means of filling space. Supposing then that the chains are sufficiently mobile and liquidlike, the system will adopt a (high-symmetry) hexagonal disposition preferentially, and so it is postulated that the arrangement within the

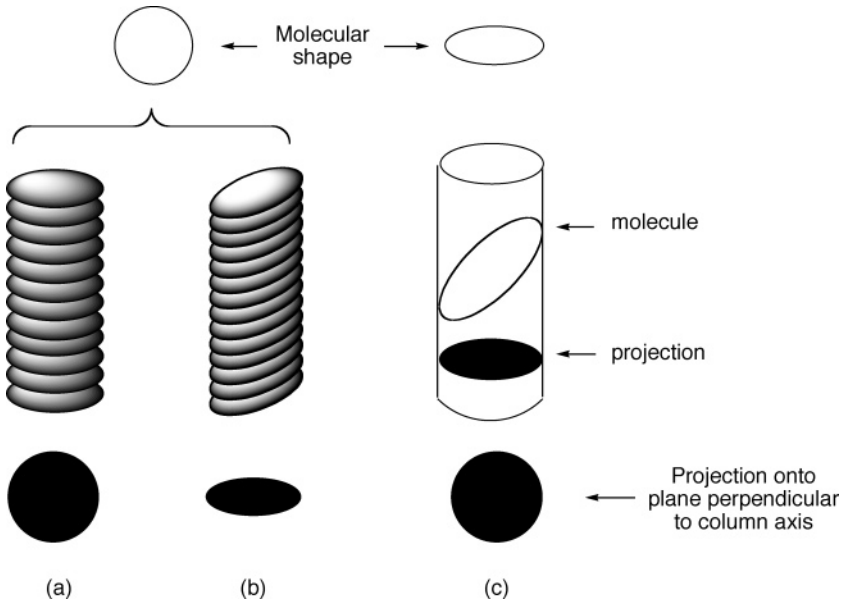

Figure 14. Figure to show how (b) elliptical cross sections may arise from circular objects in a column and (c) how circular cross sections may arise from elliptical objects in a column.

columns is driven by the mesophase symmetry and accommodated by the molten chains and the tilting of the core.

Now, while the Col_h phase of these materials requires that the molecules are tilted within the columns and while this average tilt angle must be the same from column to column, it cannot be correlated directionally from one column to the next for the optical textures observed contain homeotropic domains which requires that the phase is optically uniaxial. Correlated tilting would effectively reduce the symmetry of the phase which would mean that the phase would have to be optically biaxial and homeotropic textures would not be possible.

The overriding considerations at the Col_h-Col_r transition in these complexes is that it is second-order and it is observed that neither the columnar cross section, *s*, nor the core cross section, s_{ar}, changes discontinuously across the transition. This is in stark contrast to the situation found in certain organic polycatenar mesogens described recently where the same transition was associated to a large enthalpy change (strongly first-order transition) and there was a step change in the variation of *s*.[26]

As the Col_h-Col_r transition occurs on cooling the sample, it is proposed that it is driven by a reduction in chain mobility which does not happen isotropically; rather the mobility becomes more constrained in one direction rather than another, allowing the effective shape of the mesogen to change. However, the change in shape does not have to lead to a change in the area of the cross section. This point might be understood as follows. While the discussion has properly concentrated on the areas of circular and elliptical cross sections, geometrically speaking, it is valid to consider *s* as the area of one hexagon in the net shown in Figure 15a. Figure 15b shows that same net after a distortion, the result of which is that the regular shape of the hexagon has changed while the area of the (now irregular) hexagon has been preserved. This simple model describes a transition from *p*6*mm* to *c*2*mm* symmetry. At a molecular level, this would result from reduced chain mobility in particular directions, and so it is

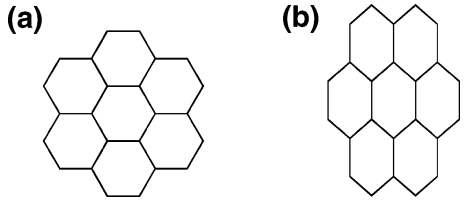

Figure 15. Distortion of a hexagonal net with retention of area.

entirely reasonable to consider that, with a complex which is an isomer of the material undergoing this transition, the reduction in chain mobility would have a different spatial profile leading to a phase of different symmetry after transition (e.g., *p*2*gg*). Such arguments are also consistent with earlier propositions in which hexagonal phase formation is accommodated by the mobility of the chains, so that as chain mobility decreases, the system cannot arrange itself to give a circular cross section and so the symmetry decreases. That the transition is driven by a reduction in chain mobility is then consistent with the observed second-order nature of the phase transition, as the reduction in mobility would not require a catastrophic change in lattice dimensions.

The final point is whether the data collected and the interpretation offered can also be used consistently to propose a model for the molecular organization within the columnar phase. Traditionally, it has been considered that, in the columnar phase of polycatenar mesogens, a number of molecules (normally three or four) form a "columnar slice" and that these "slices", which contain molecules whose long axis is considered perpendicular to the columnar axis, stack one upon another to give the columns. This model emanated from studies akin to this one in which data obtained from X-ray diffraction and from dilatometry were combined to suggest a number of molecules (or at least molecular equivalents) which exist in a "slice" of column of a particular height, *h*. In these cases, the model is supported by the observation that the columnar width in the hexagonal phase (equivalent to the hexagonal *a* parameter) is the same as the molecular length. In the present case, however, the data show that such an arrangement cannot pertain and that,

(26) Guillon, D.; Heinrich, B.; Ribeiro, A. C.; Cruz, C.; Nguyen, H. T. *Mol. Cryst. Liq. Cryst.* **1998**, *317*, 51−64.

overall, the complexes are tilted between 43° and 53° from the normal to the columnar axis *or*, alternatively, between 37° and 47° from the columnar axis itself.

It seems, therefore, that the driving force in forming the columnar phases is the efficient filling of space in the highest available symmetry and that the molecular species that make up the phase will adjust their orientation and arrangement to allow this to happen. Thus, in some cases this efficient space-filling will allow for the molecules to be perpendicular to the columnar axis (which could be regarded as an example at one extreme), whereas, in others, the molecules will need to arrange themselves at some angle to the columnar axis. While not directly comparable to the systems described here due to their bent shape, the same principles can be applied in considering the columnar phases of polycatenar dithiolium salts where it is postulated that the molecular cores are parallel with the columnar axis;[27] this method of filling space might then be regarded as the other "extreme".

High-symmetry arrangements, i.e., the hexagonal phase, will then be facilitated by some combination of flexible molecular cores and mobile terminal chains which allows the molecules to project a circular cross section onto the column, but where this is not possible, then lower symmetry phases will result. It then follows that transitions to phases of lower symmetry will be driven by loss of motional freedom in the core and/or chains in a manner similar to that described in this work.

Finally, it is appropriate to comment on the parameter N_{col} which defines the number of molecules calculated to be present in a slice of column of height, h. It is often the case in polycatenar systems that a d_{001} reflection, corresponding to the columnar repeat, is absent, whereas it is an important feature of the X-ray patterns in the columnar phases of most discotic systems. However, on occasion (for example in this work and in previous studies of related silver complexes[28]) there is evidence for a columnar repeat spacing, and in these cases, the calculation of N_{col} has some meaning. Indeed, in the present work it may be that the 9 Å spacing represents a periodicity of the strongly scattering palladium centers. Similarly, where the molecules are found to be perpendicular to the columnar axis, then h can be deduced and, once more, N_{col} can be evaluated meaningfully and, in these cases, can provide a sensible picture of phase organization. However, it is probable that the discrete "columnar slice" implied in this latter case is unique to this situation and that, in the majority of cases, a given slice of whatever height is unlikely to contain an exact number of complete molecules so that N_{col} refers to a number of complete equivalent molecules as might be found, for example, in the unit cell of a crystalline species.

Acknowledgment. We thank the EU for support (B.D.) and Johnson Matthey for generous loans of palladium salts. B.D. would like to gratefully thank Dr Anne-Marie Levelut for her helpful comments and suggestions.

Supporting Information Available: Experimental section; table of crystallographic data and of transition temperatures; illustrative X-ray diffraction patterns, optical textures, and other data as referred to in the text; cif files for the two structures. This material is available free of charge via the Internet at http://pubs.acs.org.

JA0471673

(27) Artzner, F.; Veber, M.; Clerc, M.; Levelut, A. M. *Liq. Cryst.* **1997**, *23*, 27−33.

(28) Donnio, B.; Bruce, D. W.; Heinrich, B.; Guillon, D.; Delacroix, H.; Gulik-Krzywicki, T. *Chem. Mater.* **1997**, *9*, 2951−2961.